Competition between Micro- and Macrophase Separations in a Binary Mixture of Block Copolymers. A Dynamic Density Functional Study

Hiroshi Morita,*,†,⊥ Toshihiro Kawakatsu,‡,|| Masao Doi,‡ Daisuke Yamaguchi,§ Mikihito Takenaka,§ and Takeji Hashimoto§

Japan Chemical Innovation Institute, Res. & Educ. Center, Nagoya University, Nagoya 464-8601, Japan; Department of Computational Science and Engineering, Nagoya University, Chikusa-ku, Nagoya 464−8603, Japan; Department of Polymer Chemistry, Graduate School of Engineering, Kyoto University, Sakyo-ku, Kyoto, 606-8501, Japan; Department of Physics, Tohoku University, Sendai 980−8578, Japan; and Quantum Phase Electronics Center & Department of Applied Physics, School of Engineering, The University of Tokyo, Hongo, Bunkyo-ku, Tokyo, 113-8656, Japan

Received March 15, 2002; Revised Manuscript Received May 31, 2002

ABSTRACT: Using the dynamic density functional (DDF) simulation technique, we studied the domain morphology and dynamics of phase separation in a mixture of long and short block copolymers. The simulation results well reproduce the recent results of the X-ray scattering experiment and the TEM observation on a mixture of long and short polystyrene−polyisoprene block copolymers. The DDF simulation clarifies that the three-dimensional complex domain structures and the mechanism of the dynamics of the phase separation are arising from the competition between the microphase separation and the macrophase separation.

1. Introduction

It is well-known that block copolymers show a variety of microphase-separated domain structures on the mesoscopic length scales of the order of 10−100 nm.[1−5] For the simplest example of linear diblock copolymer melts, classical phases such as lamellar, cylindrical, spherical, and gyroid phases are observed experimentally[2,3] and their stability is studied theoretically.[6−9] For linear triblock copolymer melts, much more complex microphase-separated structures are found.[10,11] In these neat block copolymer systems, the equilibrium microphase-separated structures are spatially periodic. Numerical simulations suggest, however, that intermediate metastable structures are important in the formation processes of these periodic structures.[12−14]

When two block copolymers are mixed, a macrophase separation as well as the microphase separation can take place.[5,15] In such a mixture, a rich variety of the phase behavior and the formation dynamics are expected as a result of the competition between the micro- and macrophase separations. This is because the spatial periodicity of the domains is not necessarily required for such systems. Actually, Hashimoto and co-workers reported an experimentally obtained phase diagram of a mixture of short and long diblock copolymers, where the system shows complex and nonperiodic macrophase-separated domain structures.[16−19]

Relevant theoretical works to these experiments on the binary mixture of block copolymers were reported by Shi and Noolandi[20] and by Matsen.[21] They performed one-dimensional calculations of the equilibrium interfacial structures using self-consistent field (SCF) theory and studied the phase behavior and the interfacial structures. However, these equilibrium one-dimensional studies can miss the essential features of the irregular and nonequilibrium macrophase-separated domains that are observed in the experiments, and therefore, dynamic simulations using two- and three-dimensional systems are required.

In this article, we perform a series of computer simulations using a physical model of the system experimentally studied by Hashimoto and co-workers to clarify the basic mechanism of the phase behavior and the dynamics of the domain formation. To construct such a physical model, it is indispensable to take into account of the physical properties of the system on the coarse-grained level (e.g., 10−100 nm). In the present case, they are the chain architectures (block structures), the conformational entropy (stretching elasticity) of the chains, the local phase separation between different types of segments, and the diffusion processes of the segments. To take these properties into account on the quantitative level, we adopt the dynamic density functional (DDF) theory combined with the SCF technique.[22] Although the DDF theory has been applied to various phase-separation problems,[23,24] the targets of these studies were restricted to rather simple systems, such as the block copolymer melts or the polymer blends. Hashimoto et al. have studied the competition between two microphase separations using the random phase approximation, which can be applied only to the early stage of the microphase separations.[25] On the other hand, the DDF method that we will use in the present study can be applied even to the late stage. Thus, the application of the DDF theory to the block copolymer mixtures that shows complex structures and complex dynamics can also be a good test of the validity and predictability of the theory.

This paper is organized as follows. In section 2, we summarize the phase behavior obtained by the experiment. The formulation of the DDF theory for this system

† Japan Chemical Innovation Institute, Research & Educcation Center, Nagoya University.
‡ Department of Computational Science and Engineering, Nagoya University.
§ Kyoto University.
|| Tohoku University.
⊥ The University of Tokyo.

10.1021/ma0203997 CCC: $22.00
Published on Web 08/10/2002

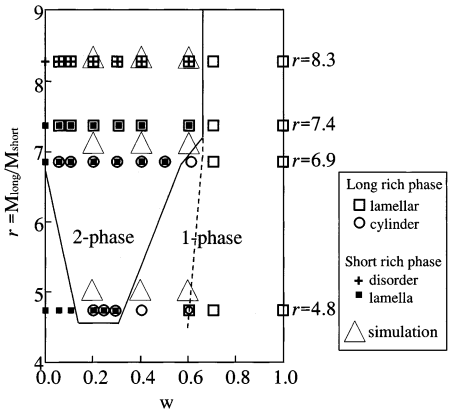

Figure 1. Experimentally obtained phase diagram of a binary mixture of long and short PS−PI diblock copolymers with w being weight fraction of the long block.

is given in section 3. Section 4 is devoted to the numerical results of the phase behavior, where we observe a rich variety of exotic domain structures that correspond to the experimental results. The formation dynamics of the domain structures are also investigated, and the results are given in section 5, where we discuss the effects of the competition between the micro- and the macrophase separations. Finally, we give a summary of the present work in section 6.

2. Experimental Results

As was already reported in refs 16−19, Hashimoto and co-workers investigated the phase behavior of a binary mixture of block copolymers. The system they studied is composed of long and short polystyrene−polyisoprene (PS−PI) diblock copolymers. The molecular weight of the long block copolymer is fixed to $M_{long} = 1.0 \times 10^5$, while that of the short block copolymer M_{short} is changed so that the ratio $r \equiv \{M_{long}\}/\{M_{short}\}$ changes within the range $4.8 \le r \le 8.3$.[18,19] The architectures of the block copolymers are specified by the block ratio defined by $f_\alpha = (\{M_{\alpha,PS}\}/\{\rho_{PS}\})\}/\{\{(\{M_{\alpha,PS}\}/\{\rho_{PS}\}) + (\{M_{\alpha,PI}\}/\{\rho_{PI}\})\}$, where α = long or short is an index specifying the long or short chains, $M_{\alpha,PS}$ and $M_{\alpha,PI}$ are the number-averaged molecular weights of the PS-block and PI-block of the α-type chain, and ρ_{PS} and ρ_{PI} are the densities of the PS- and PI-type blocks, respectively. The actual values of the block ratio of the long and short block copolymers are $f_{long} = 0.47$ and $f_{short} = 0.40-0.49$, respectively, which means that the block copolymers are slightly asymmetric.

The experimentally determined phase behavior of the binary block copolymer mixture is shown in Figure 1,[18] where the ratio r of the molecular weights of the long and short block copolymers and the weight fraction w of the long block copolymer are taken as the independent variables. In both neat phases of the long block copolymer ($w = 1.0$) and of the short block copolymer ($w = 0.0$), the slight asymmetries in the block structures ($f \neq 0.5$) do not strongly affect the domain morphology, and the lamellar structures are observed except for the shortest block copolymer ($r = 8.3$) for which only disordered phase is attained. When the two block copolymers are mixed, however, the observed domain morphologies formed by the long block copolymer are not only lamellar structures but also cylindrical ones. In this case, mixing two block copolymers enhances the slight asymmetry of the long and/or short block copolymers.

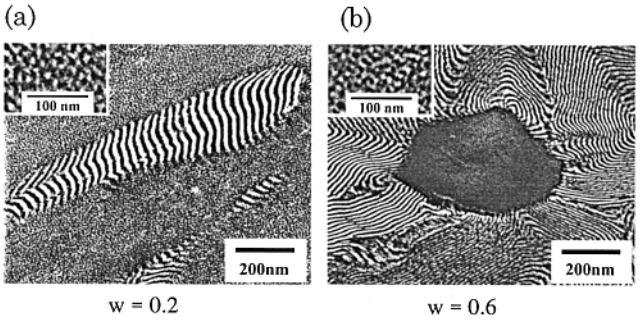

Figure 2. TEM images of the domain structures of (a) $(r,w) = (8.3, 0.2)$ and (b) $(r,w) = (8.3, 0.6)$, which indicate the macrophase separations into lamellar (rich in long blocks) and disordered phase (rich in short blocks). The insets show enlarged images of the disordered phase. The scales of each picture are also indicated.

The main target of the present study, i.e., the competition between the micro- and macrophase separations, is clearly observed in the two-phase coexistence regions. In these two-phase regions, the lamellar phase or the cylindrical phase of the long block copolymer coexists with the lamellar phase or the disordered phase of the short block copolymer. The TEM images in the two-phase regions for the cases with 20% and 60% volume fractions of the long block copolymer are shown in Figure 2, parts a and b, respectively. As is observed in Figure 2a, the microphase-separated lamellar domains rich in the long blocks are dispersed in the matrix of the uniform disordered phase formed by the short blocks. The lamellar domains do not extend over the system but are confined in closed domains created by the macrophase separation. On the other hand, the structure is inverted in Figure 2b; i.e., the disordered phase forms a globular domain in a matrix of the microphase-separated regions. These results suggest that the confinement effects may play an important role in the domain morphology formed by the micro- and macrophase separations. In the following sections, we will investigate the relation between the confinement effects and the domain morphology using computer simulations based on the DDF theory.

3. DDF Theory

To study inhomogeneous phase-separated structures in polymer systems, the DDF theory is a convenient and useful tool. The basic assumptions in the DDF theory are as follows.

(1) The chain conformations are represented by the Gaussian-chain statistics, and are described using the path integral formalism.

(2) The short-range interactions between different types of segments are introduced and are described by the so-called χ parameters.

(3) The dynamics is introduced by assuming a simple local diffusion of the segments driven by the local gradient of the chemical potential.

Assumptions 1 and 2 correspond to the long-range and the short-range interactions in block copolymer systems, and are necessary to reproduce the microphase separation behavior.[8] Assumption 3 is essential in the present study because the confined domains shown in Figure 2 are expected to be a nonequilibrium transient state created in the coarsening processes.

Now we briefly describe the mathematical formulation of the DDF theory for block copolymer systems. As

is discussed above, in the DDF theory, the local segment diffusion process is assumed to be driven by the gradient of the chemical potential. Here we introduce an index K denoting the type of the subchains, i.e., K = PS (styrene) or PI (isoprene), and use the index α defined in section 2, i.e., α = long or short, respectively. Denoting the density of the K-type segments of the α-type chain as $\phi_{K\alpha}(\mathbf{r})$, the time evolution of the set of density fields $\{\phi_{K\alpha}(\mathbf{r})\}$ is assumed to obey the following equation

$$\frac{\partial}{\partial t}\phi_{K\alpha}(\mathbf{r},t) = L_{K\alpha}\nabla^2\mu_{K\alpha}(\mathbf{r},t), \tag{1}$$

where $\mu_{K\alpha}(\mathbf{r},t)$ and $L_{K\alpha}$ are the chemical potential and the segment mobility of the K-type segments of the α-type chain. Here, we neglected the dependence of the segment mobility $L_{K\alpha}$ on the segment density $\phi_{K\alpha}(\mathbf{r})$ for simplicity. If densities of some components are very small, such neglect is not justified. In the present case shown in Figure 1, however, the amplitudes of the density modulations are rather small in the early and intermediate stages of the phase separation, where the dependence of the segment mobility ($L_{K\alpha}$) on the local segment density can be neglected. Another approximation we assumed in eq 1 is the local phantom dynamics of the chains where neither the collective motions of the whole chain nor the entanglement effects are taken into account. In the experiments shown in section 2, the time scale of the phase separation is sufficiently longer than the reptation time. This means that the individual chain dynamics due to reptation motion is not important in the dynamical model of the phase separation as long as the free energy is correctly evaluated on the basis of the local equilibrium assumption. In such a case, the Rouse dynamics assumed in eq 1 is a reasonable approximation. If the characteristic time scale of the phase separation is the same order as the individual chain dynamics, nonlocality in the segment mobility caused by the collective motion of the whole chain should be treated more carefully. In such a case, collective Rouse dynamics model[26] or the reptation dynamics model[27,28] should be used instead.

To solve the time evolution described by eq 1, we have to evaluate the chemical potential $\mu_{K\alpha}(\mathbf{r},t)$ for the given profiles of the segment density fields $\phi_{K\alpha}(\mathbf{r})$. In polymeric systems, the most important part of the chemical potential originates from the conformational entropy of the chains. To evaluate it, we use the mean-field approximation where we consider a Gaussian chain under the influence of external mean fields. We denote the mean fields acting on the K-type segments of the α-type chain as $\{V_{K\alpha}(\mathbf{r})\}$.[29] Then the partition function of such a Gaussian chain in the external fields is given by the path integrals that obey the following equation

$$\frac{\partial}{\partial s}Q_\alpha^{\pm}(\mathbf{r},s) = \left[\frac{b^2}{6}\nabla^2 + V_{K_\alpha^{\pm}(s)}(\mathbf{r})\right]Q_\alpha^{\pm}(\mathbf{r},s), \tag{2}$$

where $Q_\alpha^{\pm}(\mathbf{r},s)$ are the path integrals for the forward direction (+) and the backward direction (−) along the chain, b is the Kuhn segment size that is assumed to be the same for the styrene and the isoprene segments, and $K_\alpha^{\pm}(s)$ denotes the segment species of the sth segment of the α-type chain in the ± direction, respectively. For the present system

$$K_\alpha^{+}(s) = \begin{cases} S & (0 \le s \le J_\alpha) \\ I & (J_\alpha \le s \le N_\alpha) \end{cases} \quad \text{and}$$

$$K_\alpha^{-}(s) = \begin{cases} I & (0 \le s \le N_\alpha - J_\alpha) \\ S & (N_\alpha - J_\alpha \le s \le N_\alpha) \end{cases} \tag{3}$$

where N_α and J_α are the total number of segments per an α-type chain and the total number of segments in the PS block of the α-type chain. Equation 2 should be solved using the following initial condition

$$Q_\alpha^{\pm}(\mathbf{r},0) = 1 \tag{4}$$

Then, the segment density $\phi_{K\alpha}(\mathbf{r})$ is given by

$$\phi_{K\alpha}(\mathbf{r}) = n_\alpha \frac{\int_{K\alpha} \mathrm{ds}\; Q_\alpha^{+}(\mathbf{r},s)Q_\alpha^{-}(\mathbf{r},N_\alpha - s)}{\int d\mathbf{r}\int_{K\alpha} \mathrm{ds}\; Q_\alpha^{+}(\mathbf{r},s)Q_\alpha^{-}(\mathbf{r},N_\alpha - s)}, \tag{5}$$

where n_α is the total number of the α-type chains in the system and $\int_{K\alpha}$ ds denotes the integration over all the K-type segments of the α-type chain. The external field $V_{K\alpha}(\mathbf{r})$ is given by the sum of the segment−segment interaction and the constraining potential $\gamma_{K\alpha}(\mathbf{r})$ that forces the segment density to a given density distribution $\phi_{K\alpha}(\mathbf{r})$. Thus, the external field $V_{K\alpha}(\mathbf{r})$ is given by the following expression

$$V_{K\alpha}(\mathbf{r}) = \sum_{K'}\chi_{KK'}\{\phi_{K'\mathrm{long}}(\mathbf{r}) + \phi_{K'\mathrm{short}}(\mathbf{r})\} + \gamma_{K\alpha}(\mathbf{r}) \tag{6}$$

where $\chi_{KK'}$ is the interaction parameter for a $K-K'$ segment pair. Note that an explicit expression for the constraining potential $\gamma_{K\alpha}(\mathbf{r})$ cannot be obtained. It can be obtained only through an iteration calculation using eq 2 as is described in the following.

Equations 2−6 form a closed set of self-consistent equations. To solve it, we have to determine the constraining potential $\gamma_{K\alpha}(\mathbf{r})$ by adjusting it iteratively so that the density profiles calculated by eq 5 coincide with the current density profiles obtained by time integration of eq 1. For this reason, $V_{K\alpha}(\mathbf{r})$'s are called self-consistent fields (SCF). Physically, this self-consistent calculation means that the chain conformations are assumed to be in local equilibrium under the given density profiles. Once the set of self-consistent equations, eqs 2−6, are solved, the chemical potential for the K-type segment is given by

$$\mu_{K\alpha}(\mathbf{r}) = -\gamma_{K\alpha}(\mathbf{r}) \tag{7}$$

Substituting the chemical potential $\mu_{K\alpha}(\mathbf{r})$ into eq 1, one can integrate the equation of motion, eq 1, to update the density profiles. Here, we note that when solving eq 1, it should be supplemented by the total incompressible condition

$$\sum_K\sum_\alpha \phi_{K\alpha}(\mathbf{r},t) = \text{constant} \tag{8}$$

which produces an extra current of the segments that should be added to the right-hand side of eq 1.

4. DDF Simulations on the Phase Behavior and the Domain Structures

In this section, we try to reproduce the experimental phase behavior shown in Figure 1 using DDF simulations. As is clear from Figures 1 and 2, the morphology

of the macrophase-separated domains is expected to be irregular and nonequilibrium in the two-phase region. Therefore, the dynamical simulations in the real space based on the DDF theory are desirable.

We performed a series of simulations of the phase separation processes starting from initial uniformly mixed states. To simulate growing irregular macrophase-separated domain structures, using a large simulation system is essentially important. For this purpose, we use a 2-dimensional simulation box with 256×256 square meshes with mesh width b. Periodic boundary condition is assumed for each direction. The simulations were performed for the nine phase points specified by the open triangles in Figure 1, i.e., $(r,w) = (8.3, 0.2)$, (8.3, 0.4), (8.3, 0.6), (7.1, 0.2), (7.1, 0.4), (7.1, 0.6), (5.0, 0.2), (5.0, 0.4), and (5.0, 0.6). To simulate these systems, we model the long block copolymer having a chain of length $N_{\text{long}} = 100$ composed of a PS block of length 46 and a PI block of length 54. On the other hand, the short block copolymer is modeled as a symmetric block copolymer chain of length $N_{\text{short}} = 12$ (PS:PI = 6:6) for the cases with $r = 8.3$, $N_{\text{short}} = 14$ (PS:PI = 7:7) for the cases with $r = 7.1$ or $N_{\text{short}} = 20$ (PS:PI = 10:10) for the cases with $r = 5.0$, respectively. The χ-parameter values are set to $\chi_{\text{PS,PS}} = \chi_{\text{PI,PI}} = 0.0$ and $\chi_{\text{PS,PI}} = 0.5$ so that the order−disorder (lamellar−disorder) transition points evaluated for the neat block copolymer systems roughly coincide with those of the experimental transition points**.** As the block copolymers used in the experiments have fluctuations in the degree of asymmetry between the two blocks, the coincidence between the theoretical and experimental phase diagrams can be achieved only within a certain error level.[18] We here note that in a real system the position of the critical point of the microphase separation deviates from its mean field prediction by an amount proportional to $N^{-1/3}$ due to the fluctuation effect.[30] Because there is no experimental data for the mobility in eq 1, we assumed that they are the same for all the segment species, i.e., $L_{K\alpha} = 1.0$, for simplicity. The integration of the evolution equation, eq 1, is performed with the usual Euler difference scheme with time mesh width $\Delta t = 0.1$, and the simulations were performed up to 50 000 time steps (up to $t = 5000$) for each parameter set.

4.1. Domain Morphology. In Figures 3 and 4, typical time evolutions of the domain structures obtained by the two-dimensional DDF simulations are shown for the two cases $(r,w) = (5.0, 0.6)$ and $(r,w) = (8.3, 0.2)$, respectively. In each figure, the upper pictures show the density distribution of segments (both styrene and isoprene segments) belonging to the long block copolymer, and the lower pictures show that of the styrene segments belonging to both long and short block copolymers. In these figures, the bright regions indicate the high-density regions of the long block copolymer and those of the styrene segments, respectively. In Figure 3, the contrast of the lower pictures is clearer than that of the upper ones, which indicates strong separation between isoprene segments (PI) and styrene segments (PS). On the other hand, in the upper pictures, the narrow gray stripes indicate the region where the long chains are excluded due to adsorption of the short chains at the PI−PS interfaces. According to the experimental phase diagram given in Figure 1, the simulation system in Figure 3 is expected to show a single phase with the cylinder or lamellar structure composed of both short and long block copolymers. The final structure obtained by the DDF simulation ($t = 5000$) actually shows a single phase with the lamellar morphology more or less consistently with the experimental results, although the DDF result contains many defects.

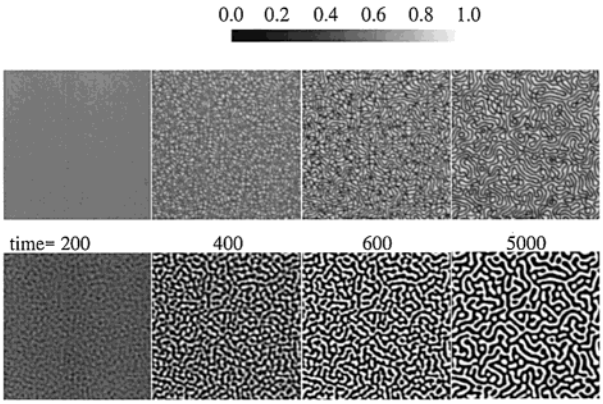

Figure 3. Typical time evolutions of the domain structures obtained by the two-dimensional DDF simulations are shown for the case $(r,w) = (5.0, 0.6)$ at times $t = 200$, 400, 800, and 5000, respectively. The upper figures are the snapshot pictures of the density distribution of segments belonging to the long block copolymer, and the lower figures to those of the distribution of the styrene segments belonging to both long and short block copolymers. The dark and bright regions indicate the low and high-density regions, respectively.

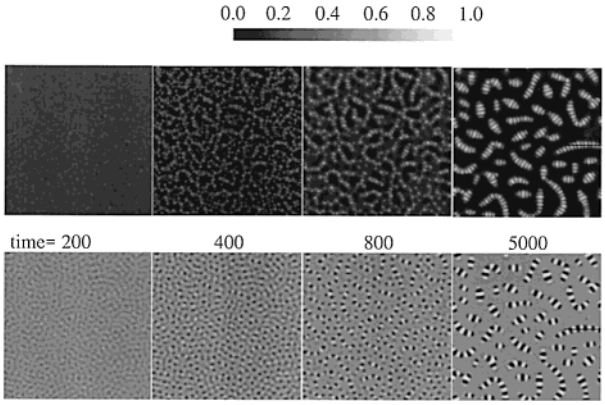

Figure 4. Similar snapshot pictures as those in Figure 3 but for the case $(r,w) = (8.3, 0.2)$.

The situation becomes more complex for the case in Figure 4. The experimental result predicts a macrophase separation showing a coexistence of a lamellar phase of the long block copolymer and a disordered phase of the short block copolymer. As is shown in Figure 4, the domain structure obtained by the DDF simulation is composed of many islands of lamellar domains immersed in a matrix of the disordered phase. A detailed analysis of the composition in each region showed that the lamellar domains are mainly composed of the long block copolymer while the disordered matrix is composed of the short block copolymer. Thus, in this case, a macrophase separation between the long and the short block copolymers causes the island-matrix structure. In this structure, we cannot observe any preferential wetting of PS or PI blocks of the long block copolymers at the interface between the island and the matrix (macrointerface), as in the case of the macrophase separation in the mixtures of PS−PI and homopolystyrene,[37] because the short chains in the disordered state (matrix) act as a nonselective solvent for the long chains. Thus, the microinterface between the PS and PI lamellae is perpendicular to that of the macrointer-

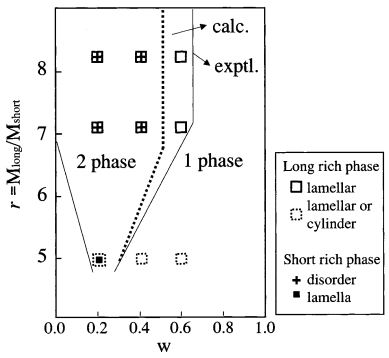

Figure 5. Comparison between the experimental phase diagram and the corresponding results of the two-dimensional DDF simulations.

face. The shape of the island domain is elongated in the direction normal to the microinterfaces (the longitudinal direction) rather than in the direction parallel to them (the lateral direction). This is due to the anisotropy in the interfacial free energy of the macrointerface, that is, the interfacial energy of the interface parallel to the longitudinal direction is smaller than that parallel to the lateral direction. These results are consistent with the experimental ones in Figure 2 and those in refs 31 and 32.

As is shown in Figures 3 and 4, the domain morphology seems to be strongly influenced by the dynamics of their formation process. A detailed analysis on the dynamics of the phase separation will be given in section 5 using the scattering function.

4.2. Phase Diagram. For the other sets of parameters, the results of the two-dimensional DDF simulations are shown in Figure 5. We can confirm that the DDF simulation reproduces the experimental phase behavior quite well, except for the discrepancy in the position of the boundary between the two-phase region (lamellar + disorder) and the one-phase region (lamellar or cylindrical) around $w \cong 0.6$. (cf. the two boundaries drawn by the thick (simulation) and thin (experiments) lines.) Thus, we conclude that the real-space DDF simulation can predict the phase behavior of complex polymer systems even if we do not know the candidates of the domain structures a priori. The discrepancy between the theory and the experiment around $w \cong 0.6$ originates from the difference in the dimensionality. In the two-dimensional simulations, the lamellar phase is artificially stabilized because the instability associated with the undulations of the layers in the third direction is prohibited.

4.3. Three-Dimensional Domain Structures. Although large-scale two-dimensional DDF simulations can reproduce the overall phase behavior, there are certain properties that cannot be captured in two-dimensional simulations. One such example is the three-dimensional fine structures of the island domains observed in Figure 4. A similar situation takes place in the TEM observations for the real system (see Figure 2), in which only two-dimensional pictures of the cross sections are obtained. To clarify the fine structures of the island domains in Figure 4, we performed three-dimensional real-space static SCF simulations using the same parameters as those in Figure 4 but with $30 \times 30 \times 30$ meshes, and the result is shown in Figure 6, parts a and b. (Here, "static simulation" means a simulation searching for the local minimum of the free energy.) As is shown in Figure 6, parts a and b, the domain

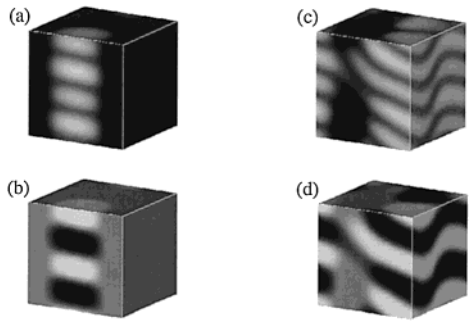

Figure 6. Results of three-dimensional simulations are shown.Parts a and b are for the same system as shown in Figure 2a (i.e., Figure 4). Part a shows the density distribution of segments belonging to the long block copolymer, and part b shows those of the distribution of the styrene segments belonging to both long and short block copolymers, respectively. The dark and bright regions indicate the low and high-density regions, respectively. Parts c and d are similar snapshot pictures but for the case $(r,w) = (8.3, 0.4)$, whose structure corresponds to that shown in Figure 2b.

structure is a pile of alternative arrays of oblate-shaped domains of PS-rich phase and PI-rich phase, which we named the "piled pancake" structure. The simulation conditions for the cases shown in Figures 4 and 6, such as volume fractions, block ratios, and χ parameters, are chosen so that the simulations correspond to the experimental situation shown in Figure 2a (or equivalently Figure 4). Both the two-dimensional images shown in Figures 2 and 4 and the three-dimensional image in Figure 6, parts a and b, show the same domain morphology, i.e., lamella domains confined in a prolate ellipsoidal or a cylindrical grain in the disordered bulk phase. A similar structure has also been found in an A−B block copolymer and C homopolymer mixture by Ohta and Ito using two-dimensional simulations of time-dependent Ginzburg-Landau type model.[33] On the other hand, parts c and d of Figure 6 are for the case shown in Figure 2b. One can confirm that, compared with the case in Figure 6, parts a and b, the lamellar domains and the disordered matrix are inverted. However, the lamellar domains are not flat but undulating, forming a screw dislocation whose core region corresponds to the disordered domain. As was pointed out by Groot et al.,[13,34] a screw dislocation in a lamellar domains can be artificially stabilized by the finite size effect of the simulation system. Considering the fact that the core of a screw dislocation tends to have a high pressure, the phase separation in such a core region is suppressed. Thus, the possibility of the artificial stabilization of the screw dislocation may affect the above argument on the correspondence between the two-dimensional simulations (Figure 2b) and the three-dimensional simulations (Figure 6, parts c and d) for this case.

It will be worthwhile to mention that using the three-dimensional DDF simulations we found not only the "piled pancake" structure shown in Figure 6, parts a and b, but also "tilted pancake" and "helical slider" structures. The difference between the latter two structures is caused by the external force such as the elongation force along the axis of the cylindrical region. The mechanism and the details of the formation of these exotic structures will be discussed in separate publications.[35,36]

In the formation processes of the domains shown in Figure 6, parts a−d, the competition between the macrophase separation and the microphase separation

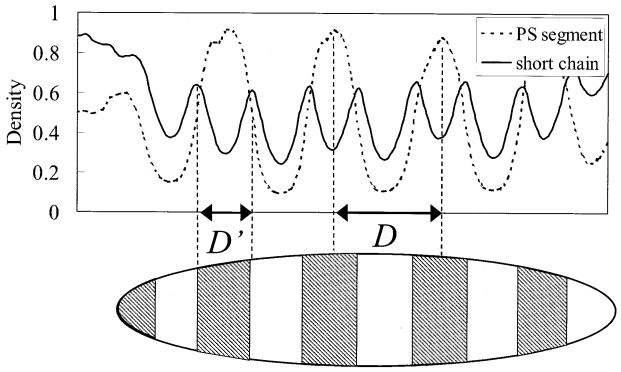

Figure 7. Total density profile of styrene segments and that of short block copolymers along the line indicated in Figure 4 are shown with a schematic picture of a lamella domain. The density difference between the short block copolymer and the long block copolymer has a period (D') that is half of the periodicity (D) of the lamellar domains.

must be important. Such a competition will further be studied in section 5.

4.4. Surface Enrichment. The chemical junctions of the short block copolymers can share the common interface with those of the long block copolymers. Because of such a behavior, the short block copolymer is called the cosurfactant to the long block copolymer. Then, the accumulation of the short block copolymers at the interface is usually called the "surface enrichment". These properties are also observed in the static SCF calculation done by Shi and Noolandi[20] and by Matsen.[21]

We can confirm this surface enrichment in the simulation data by showing the segment density profiles in a typical domain. In the upper figure of Figure 7, we show the segment density profiles along the major axis of the prolate ellipsoidal grain in Figure 4 (the case with $(r,w) = (8.3,0.2)$), which is indicated by the line in the last picture of Figure 4. The solid curve shows the segment density of the short chains, and the broken curve that of the styrene (S) segments belonging to either the long or short block copolymers. One can recognize that the long block copolymer forms a lamellar domain, and the short block copolymer is adsorbed on the interface of this lamellar domain, which lowers the interfacial tension of the lamellar interface as a cosurfactant.[20] One can also observe that the average density of the short block copolymer inside the lamellar domain is lower than that in the matrix phase, which means that the short block copolymer is excluded from the lamellar domain as a result of the macrophase separation between the long and short block copolymers. The lower figure of Figure 7 is a schematic picture of the lamellar domain that corresponds to the density profiles. The period of the peaks in the density distribution of short chains (D') is half of that of the lamellar periodicity (D); i.e., the relation $D = 2D'$ holds for this lamellar structure. This relation and the cosurfactant nature of the short block copolymer will play an important role in the dynamical analysis on the scattering function described in the next section.

Using the strong segregation theory of a lamellar phase of a block copolymer, the free energy per unit volume is roughly evaluated as

$$\frac{F}{V} = A\left(\frac{D}{N}\right)^2 + \frac{B}{D}, \tag{9}$$

where F and V are the total free energy and the total volume of the system, N is the total number of segments per a long block copolymer chain, D is the lamellar periodicity, and A and B are constants. The first term on the right-hand side of eq 9 is the elastic energy associated with the chains, while the second term accounts for the interfacial free energy where B is proportional to the interfacial tension σ. The equilibrium lamellar periodicity D^* is obtained by minimizing eq 9 with respect to D, which leads to

$$D^* = \left(\frac{B}{2A}\right)^{1/3} N^{2/3} \tag{10}$$

Because of the relation $B \propto \sigma$, the reduction in the interfacial tension σ due to the surface enrichment results in a decrease of the lamellar thickness. Thus, we can conclude that the lamellar periodicity is a decreasing function of the amount of the short block copolymers accumulated at the interfaces. This feature will be discussed in the next section.

5. DDF Simulations on the Dynamics of Phase Separation

One of the advantages of the DDF simulations is that we can study the mechanism of the formation of the final complex domain structures. The model dynamics described by eq 1 corresponds to the slow diffusion motion of the segments driven by the local chemical potential gradient. The effects of the connectivity constraint of the chain are taken into account through the chemical potential $\mu_{K\alpha}(\mathbf{r},t)$ evaluated using the path integral.

To discuss the phase separation dynamics quantitatively, we calculated the circularly averaged scattering functions for the following two-order parameters $X(\mathbf{r})$:

$$X(\mathbf{r}) \equiv \begin{cases} \phi_{PS} - \phi_{PI} \equiv (\phi_{PSlong} + \phi_{PSshort}) - (\phi_{PIlong} + \phi_{PIshort}) \\ \phi_{long} - \phi_{short} \equiv (\phi_{PSlong} + \phi_{PIlong}) - (\phi_{PSshort} + \phi_{PIshort}) \end{cases} \tag{11}$$

In principle, both of these order parameters are affected by the microphase separation and the macrophase separation. However the former describes the phase separation between the PS phase and the PI phase, i.e., the microphase separation, while the latter describes the macrophase separation between the long and short block copolymers. The circularly averaged scattering function of an order parameter $X(\mathbf{r})$ is defined using its Fourier transform $\tilde{X}(\mathbf{q})$ as

$$S_X(q) \equiv \frac{1}{4\pi}\int_{|\mathbf{q}|=q} d\Omega \langle|\tilde{X}(\mathbf{q})|^2\rangle \tag{12}$$

where $\int_{|\mathbf{q}|=q} d\Omega$ means the integration over the solid angle Ω of the wave vector $\mathbf{q}$ keeping the magnitude of $\mathbf{q}$ at a certain value q, and the angular bracket $\langle\ \rangle$ means the ensemble average over the domain configurations.

We calculated the time evolutions of the circularly averaged scattering functions for the two-order parameters (a) $\phi_{PS} - \phi_{PI}$ and (b) $\phi_{long} - \phi_{short}$ defined by eq 11 for the two cases given in Figures 3 and 4, i.e., $(r,w) = (5.0, 0.6)$ and $(8.3, 0.2)$, respectively. The results are, respectively, shown in Figures 8 and 9 on semilogarithmic scales, where the wavenumber q is scaled by the position of the main peak q_m of $\phi_{PS} - \phi_{PI}$ at the final time step ($t = 5000$). In Figure 9, there is a shoulder in

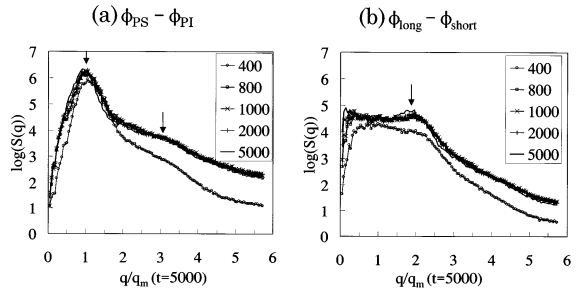

Figure 8. Time evolutions of the circularly averaged scattering functions for the two order parameters (a) $\phi_{PS} - \phi_{PI}$ and (b) $\phi_{long} - \phi_{short}$ for the case given in Figure 3, i.e., with $(r,w) = (5.0, 0.6)$ shown on semilogarithmic scales. From the bottom to the top, the times are $t = 400$, 800, 1000, 2000, and 5000, respectively. Arrows indicate peaks and shoulders. The wavenumber q is scaled by the peak position q_m at $t = 5000$.

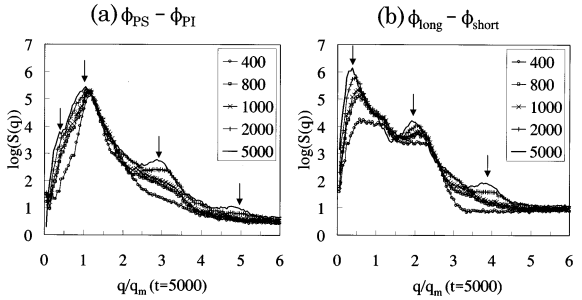

Figure 9. Similar to Figure 8 but for the case in Figure 4, i.e., with $(r,w) = (8.3, 0.2)$ shown.

the lower wavenumber side of the main peak of ln $S(q)$. This shoulder may cause a shift of the position of the main peak. We evaluated the correct position of the main peak $q_m$by fitting the data of $S(q)$ in the interval $0 \le q \le 30(\{2\pi\}/\{L\})$ by two Gaussian peaks using the least-squares fitting method, where L is the side length of the simulation box.

Parts a and b in Figure 8 show the time evolution of the scattering functions for the formation of the lamellar phase shown in Figure 3. One recognizes a main peak in both parts a and b of Figure 8. Figure 8a shows the microphase separation between PS and PI components, giving rise to the main peak at $q \cong q_m$ and a subpeak of the higher order harmonic at $q \cong 3q_m$. The latter subpeak indicates an ordering of PS and PI lamellae with nearly identical volumes comprised of both the long block copolymers and the short block copolymers. The growth of the higher order harmonic peaks means a continuous sharpening of the interfaces between the lamellar domains while the steady main peak indicates that the spatial arrangement of the lamellar domains already exists in the early stage of the phase separation. Figure 8b reflects the microphase separation between (or spatial variation of) the short and long block copolymers. The main peak position in Figure 8b is twice as large as that in Figure 8a, reflecting a half of the lamellar periodicity. This is reasonable because according to the discussions in section 4.4, the density distribution of the short block copolymer in the lamellar morphology has a period that is a half of the lamellar periodicity. Similar behavior is also observed in the island domain in Figure 4 as was discussed in section 4.4. Thus, the main peak in Figure 8b shows the existence of the surface enrichment of the short block copolymers at the interfaces of the lamellar domains formed by the long block copolymers. Note that the positions of the main peaks in both parts a and b of Figure 8 do not significantly shift with time. Therefore, the periodicity of the lamellar layers is almost fixed in the early stage of the ordering process. According to the discussion in section 4.4, this means that the amount of the surface enrichment of the short block chains is almost constant throughout the simulation time in this one-phase region of the lamellar phase.

The situation drastically changes in the other case given in Figure 9, parts a and b. In Figure 9a, we can observe three peaks at $q \cong q_m$, $3q_m$, and $5q_m$ and a growing shoulder in the small q-region where $q < q_m$. Here, the small deviation in the positions of the peaks from $q = 3q_m$ and $5q_m$ may be due to the finite system size effect that enhances the scattering intensity in the small wavenumber region and causes an overestimate of the wavenumber of the main peak. Similar to the situation in Figure 8a, the former three peaks correspond to the lamellar ordering of a symmetric block copolymer. The fact that only the scattered intensities of the subpeaks at $q \cong 3q_m$, and $5q_m$ grow indicates that the microphase-separated structure is already formed in the early stage, and the interfaces are becoming sharper and sharper as the time goes on. On the other hand, the growth of the shoulder around $\{q\}/\{q_m\} \approx 0.3-0.7$ in Figure 9a and the corresponding growing peak in Figure 9b at $\{q\}/\{q_m\} \approx 0.3-0.7$ indicate that the macrophase separation between short and long block copolymers takes place. We observe growth and shift of this peak to the lower wavenumber side as the time goes on, which is characteristic of the coarsening process of macrophase separation.

In Figure 9b, the peak around $q \approx 2q_m$ corresponds to the microphase separation. This indicates that the periodicity corresponding to this peak is half of that of the main peak in Figure 9a. We recognize that this peak for the microphase separation in Figure 9b is slightly shifting to the smaller wavenumber side as the phase separation proceeds. Such a coarsening of the lamellar domain can be understood as follows. As was discussed in section 4.4, the short block copolymers are gradually excluded from the lamellar domains and dissolve to the disordered matrix. Such a decrease in the surface enrichment of the short block copolymers enhances the interfacial tension, leading to the coarsening of the lamellar domains as is expected by eq 10. This argument does not contradict with the calculation by Shi and Noolandi,[20] who showed that addition of small amount of short block copolymer to a lamellar phase of a long block copolymer causes a decrease in the interfacial free energy and a decrease in the period of the lamella layers. These results suggest, within our assumption of the constant segment mobility, the following mechanism of the phase separation. First a local phase separation between PS and PI segments takes place, and then both the macrophase separation and lamella ordering proceed.

6. Concluding Remarks

In this article, we reported the results of two- and three-dimensional real space DDF simulations of a binary mixture of short and long block copolymers. We confirmed that the two-dimensional DDF simulations well reproduce the phase diagram experimentally obtained by Hashimoto and co-workers.[16−19] A three-dimensional simulation revealed the details of the domain structures produced by the competition between

the macro- and microphase separations. Such information is important in constructing the three-dimensional structures from the TEM images of the two-dimensional cross sections.

Dynamics of the phase separation was also studied using the DDF simulations. The temporal evolution of the scattering functions suggests that the microphase separation and the macrophase separation proceed cooperatively. We also found that the coarsening of the macrophase-separated domains takes place at the same time of the change in the surface enrichment of the short chains at the lamellar interfaces.

We expect that the real space DDF simulation technique will be a powerful tool to study both equilibrium and dynamic properties of similar multicomponent polymeric systems where the coexistence or the competition between two types of phase separations takes place.

Acknowledgment. This work is supported by a national project, which has been entrusted to the Japan Chemical Innovation Institute (JCII) by the New Energy and Industrial Technology Development Organization (NEDO) under METI's Program for the Scientific Technology Development for Industries that Creates New Industries. This work is in part supported by the Scientific Research Fund of the Ministry of Science, Sports and Culture, Japan (A1230 5060).

References and Notes

(1) Khandpur, A. K.; Forester, S.; Bates, F. S.; Hamley, I. W.; Ryan, A. J.; Bras, W.; Almdal, K.; Mortensen, K. *Macromolecules* **1995**, *28*, 8796.
(2) Hamley, I. W. *The Physics of Block Copolymer*s; Oxford University Press: Oxford, England, 1998.
(3) Bates, F. S.; Fredrickson, G. H. *Phys. Today* **1999**, *52*, 32.
(4) Hashimoto, T. In *Thermoplastic Elastomers, A Comprehensive Revie*w; Legge, N. R., Holden, G., Schroeder, H. E., Eds.; Hanser: Munich, Germany, 1996; p 429.
(5) Hasegawa, H.; Hashimoto, T. In *Comprehensive Polymer Science, Second Supplemen*t; Aggarwal, S. L., Russo, S., Vol. Eds.; Pergamon: New York, 1996; p 497.
(6) Helfand, E.; Wasserman, Z. R. *Macromolecules* **1976**, *9*, 879.
(7) Leibler, L. *Macromolecules* **1980**, *13*, 1602.
(8) Ohta, T.; Kawasaki, K. *Macromolecules* **1986**, *19*, 2621.
(9) Matsen, M. W.; Schick, M. *Phys. Rev. Lett.* **1994**, *72*, 2660.
(10) Krappe, U.; Stadler, R.; Voigt-Martin, I. *Macromolecules* **1995**, *28*, 4558.
(11) Zheng, W.; Wang, Z.-G. *Macromolecules* **1995**, *28*, 7215.
(12) Groot, R. D.; Madden, T. J. *J. Chem. Phys.* **1998**, *108*, 8713.
(13) Groot, R. D.; Madden, T. J.; Tildesley, D. J. *J. Chem. Phys.* **1999**, *110*, 9739.
(14) Qi, S.; Wang, Z.-G. *Phys. Rev. E* **1997**, *55*, 1682.
(15) Hashimoto, T.; Tanaka, H.; Hasegawa, H. In *Molecular Conformation and Dynamics of Macromolecules in Condensed System*s; Nagasawa, M., Ed.; Elsevier: Amsterdam, 1988; p 257.
(16) Hashimoto, T.; Yamasaki, K.; Koizumi, S.; Hasegawa, H. *Macromolecules* **1993**, *26*, 2895.
(17) Koizumi, S.; Hasegawa, H.; Hashimoto, T. *Macromolecules* **1994**, *27*, 4371.
(18) Yamaguchi, D.; Hashimoto, T. *Macromolecules* **2001**, *34*, 6495.
(19) Yamaguchi, D.; Hasegawa, H.; Hashimoto, T. *Macromolecules* **2001**, *34*, 6506.
(20) Shi, A.-C.; Noolandi, J. *Macromolecules* **1994**, *27*, 2936.
(21) Matsen, M. W. *J. Chem. Phys.* **1995**, *103*, 3268.
(22) Fraaije, J. G. E. M. *J. Chem. Phys.* **1993**, *99*, 9202.
(23) Zvelindovsky, A. V.; Sevink, G. J. A.; van Vlimmeren, B. A. C.; Maurits, N. M.; Fraaije, J. G. E. M. *Phys. Rev. E* **1998**, *57*, R4879.
(24) Morita, H.; Kawakatsu, T.; Doi, M. *Macromolecules* **2001**, *34*, 8777.
(25) Hashimoto, T.; Koizumi, S.; Hasegawa, H. *Macromolecules* **1994**, *27*, 1562.
(26) Mourits, N. M.; Fraaije, J. G. E. M. *J. Chem. Phys.* **1997**, *107*, 5879.
(27) Kawasaki, K.; Sekimoto, K. *Macromolecules* **1989**, *22*, 3063.
(28) Kawakatsu, T. *Phys. Rev. E* **1997**, *56*, 3240.
(29) Fleer, G. J.; Cohen Stuart, M. A.; Scheutjens, J. M. H. M.; Cosgrove, T.; Vincent, B. *Polymers at Interfaces*; Chapman & Hall, London, 1993.
(30) Fredrickson, G. H.; Helfand, E. *J. Chem. Phys.* **1987**, *87*, 697.
(31) Sakamoto, N.; Hashimoto, T. *Macromolecules* **1998**, *31*, 3185.
(32) Hashimoto, T.; Sakomoto, N.; Koga, T. *Phys. Rev. E* **1996**, *54*, 5832.
(33) Ohta, T.; Ito, A. *Phys. Rev. E* **1995**, *52*, 5250.
(34) Groot, R. D.; Madden, T. J. In *Structure and Dynamics in the Mesoscopic Domain*; Kulkarni, B. D., Lal, M., Eds.; Imperial College Press: London; 1998.
(35) Morita, H.; Kawakatsu, T.; Doi, M.; Yamaguchi, D.; Takenaka, M.; Hashimoto, T. Submitted for publication.
(36) Hashimoto, T.; Mitsumura, N.; Yamaguchi, D.; Takenaka, M.; Morita, H.; Kawakatsu, T.; Doi, M. *Polymer* **2001**, *42*, 8477.
(37) Koizumi, S.; Hasegawa, H.; Hashimoto, T. *Macromolecules* **1994**, *27*, 6532.

MA0203997